Overview of the Development of Design Recommendations for Eccentrically Braced Frame Links with Built-Up Box Sections

JEFFREY W. BERMAN and MICHEL BRUNEAU

ABSTRACT

Among the new additions to the 2010 AISC *Seismic Provisions* are design requirements for eccentrically braced frame links with built-up box sections. Such links do not require lateral bracing in many cases because built-up box shapes have superior lateral torsional stability relative to wide flange sections. The 2010 *Seismic Provisions* include requirements for built-up box link flange width-to-thickness ratio and other important design considerations. However, the limits on web width-to-thickness ratio default to those used for built-up box beams or columns and are inadequate for links with large inelastic shear and compression strains. Such limits are important for preventing web buckling under shear and/or flexural compression. This paper presents an overview of research on the design and behavior of links with built-up box sections, including the development of recommendations for web width-to-thickness limits and corresponding web stiffener spacing requirements and flange width-to-thickness limits for these link sections. The highlighted research program included derivation of design requirements based on plate buckling considerations; a full-scale, single-story eccentrically braced frame test; a parametric study on the impact of link cross-sectional parameters on link inelastic rotation capacity; and a series of large-scale tests on isolated links.

Keywords: eccentrically braced frames, built-up box sections, links, width-to-thickness limits.

INTRODUCTION

New design requirements for eccentrically braced frame (EBF) links with built-up box sections now appear in the 2010 AISC *Seismic Provisions* (AISC, 2010). Prior to this edition, the *Seismic Provisions* only addressed design and detailing requirements for links with I-shaped cross-sections. Built-up box links may be desirable for a number of practical situations because they have much a larger resistance to lateral torsional buckling than I-shaped links. In many cases, this eliminates the need for link lateral bracing beyond that provided by the eccentric braces. For example, when EBFs are used in elevator cores or stairwells, it may be difficult to laterally brace I-shaped links as required to prevent lateral buckling, whereas built-up box sections may be used without the need for additional lateral bracing.

The 2010 *Seismic Provisions* address most of the design and detailing considerations for EBFs with built-up box links, including the design link shear strength, link stiffener requirements, and welding requirements. However, the flange width-to-thickness requirements and web width-to-thickness requirements for built-up box links are, by default, those for built-up box shapes used as beams or columns in Table D1.1 of the 2010 AISC *Seismic Provisions,* and Section F3.5b requires that the limits for highly ductile members be used. For links in EBFs, the compressive strains in the flanges are generally lower than those for moment frames, and flange buckling is less of a concern, especially for short links. Limits on the web width-to-thickness ratio for built-up box links are important to inhibit web buckling prior to achieving the required inelastic link rotation level. As discussed later, the webs of built-up box links may be subjected to large shear stresses when the links are short and the behavior is dominated by shear yielding. In these cases, web stiffeners are effective for inhibiting web buckling when the web width-to-thickness is large. When links are longer and the inelastic flexural behavior plays a more important role, the webs may have large flexural compression stresses, and web stiffeners are ineffective in preventing web buckling. Thus, to inhibit web buckling and ensure the links can achieve the desired ductility, it is necessary to have web width-to-thickness ratio limits that address these different conditions. Bruneau (2013) provides recommended web width-to-thickness ratio limits that are a result of the research briefly reviewed here.

To develop the design recommendations for links with built-up box sections, a study was conducted that included derivation of local buckling prevention requirements from plate buckling considerations and development of link plastic strength equations; a large-scale experiment on a single-story EBF with a built-up box section; parametric finite

Jeffrey W. Berman, Ph.D., Associate Professor, Department of Civil and Environmental Engineering, University of Washington, Seattle, WA. E-mail: jwberman@uw.edu

Michel Bruneau, P.Eng., Professor, Department of Civil and Environmental Engineering, University at Buffalo, Buffalo, NY (corresponding author). E-mail: bruneau@buffalo.edu

element analyses of links with various sections; and large-scale testing of isolated links to evaluate the final design recommendations. A brief overview of these studies is provided here. Emphasis is placed on the development of recommendations for link width-to-thickness limits and web stiffener requirements—the key issues pertinent to designers who may wish to use links with built-up box sections.

LINK DESIGN EQUATIONS

Link Strength

Figure 1 shows a schematic of an EBF link with length, e, and a built-up box cross-section that consists of four plates welded together with external (Figure 1b) or internal (Figure 1c) stiffeners at a spacing, a. For links with doubly symmetric cross-sections of this type, the plastic flexural capacity, M_p, is given by

$$M_p = F_{yf} t_f \left(b_f - 2t_w \right) \left(d - t_f \right) + F_{yw} \frac{t_w d^2}{2} \qquad (1)$$

where t_w is the web thickness, t_f is the flange thickness, d is the section depth, b_f is the section width, F_{yf} is the yield strength of the flange plate material and F_{yw} is the yield strength of the web plate material. Figure 1 also identifies the free flange width, b, and the free web depth, h. The plastic shear strength, V_p, is

$$V_p = \frac{2}{\sqrt{3}} F_{yw} t_w \left(d - 2t_f \right) \qquad (2)$$

Similar to links with wide flange sections, the link length, e, plastic moment strength and plastic shear strength can be used to determine whether links will yield predominantly in shear, flexure or a mix of both. Links with $e \leq 1.6 \ (M_p/V_p)$ will yield primarily in shear and are denoted "shear links"; links with $e \geq 2.6 \ (M_p/V_p)$ will yield primarily in flexure and are denoted "flexural links"; links with lengths between those bounds will yield in a combination of shear and flexure and are denoted "intermediate links." Note that Berman and Bruneau (2005) derived expressions for shear and flexural strength that accounted for shear-flexural interaction. However, test results reported in Berman and Bruneau (2006) showed that even intermediate links were able to simultaneously achieve both their plastic shear and flexural strengths due to strain hardening. Similar observations were made for I-shaped links by Roeder and Popov (1978) and Kasai and Popov (1986). Thus, the *Seismic Provisions* neglect shear-flexural interaction for links of all lengths and cross-sections.

Link Flange Width-to-Thickness Ratio

To achieve ductile link behavior, it is necessary to delay the onset of flange local buckling until significant inelastic rotation has been achieved. Flange local buckling can cause strength degradation, precipitate flange fracture and also trigger web or lateral torsional buckling. Limiting flange width-to-thickness ratios (b_f/t_f) were derived by Kasai and Popov (1986) for EBF links with I-shaped cross-sections, and a similar derivation is used with necessary modifications
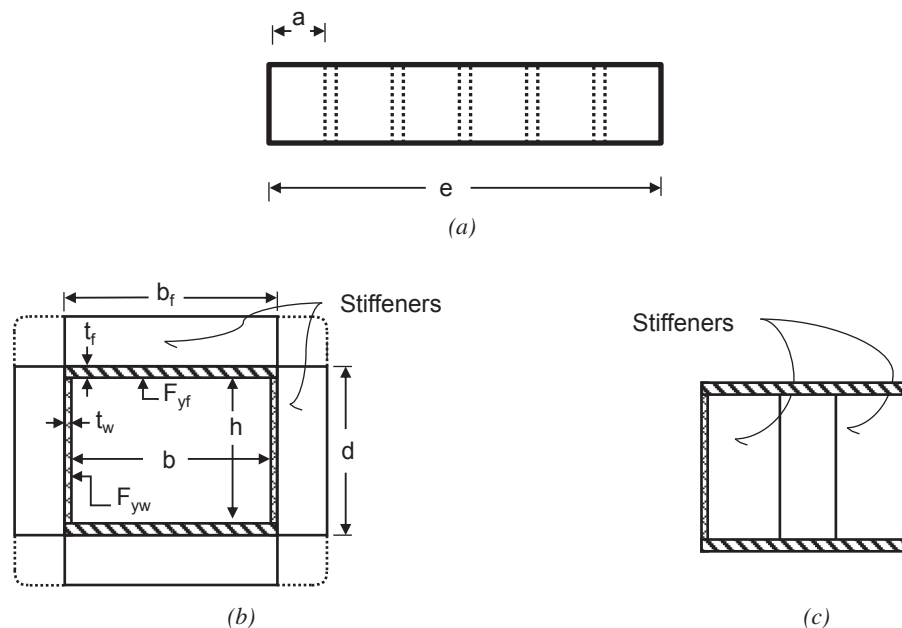

Fig. 1. (a) Link layout and stiffener spacing; (b) cross-section with external stiffeners; (c) link cross-section with internal stiffeners.

specific to built-up box sections. First the flange yield length is determined, which is the length of flange from the link end expected to yield; then the maximum flexural or shear strength of the link is achieved. This value is then introduced in a plastic plate buckling equation to determine the critical buckling stress of the flange element, which in turn is compared with an estimate of the average flange stress in the flange yield zone.

To determine the flange yield length for a general case of unequal link end moments and the presence of an axial load, Kasai and Popov (1986) used the link free-body diagram and moment diagram shown in Figure 2, where M_A and M_B are the end moments at the right and left ends, respectively, with M_A being greater than or equal to M_B and also greater than the plastic moment capacity of the link M_p because of strain hardening; V is the link shear force; α is the ratio of link axial force to link shear force; e_i is the distance from the right link end to the inflection point; l_y is the flange yield length; and γ is the link rotation angle. Using the free-body diagram of Figure 2, the plastic moment capacity of the link accounting for a reduction due to axial load but neglecting any reduction due to shear, M_{pa}, can be written as

$$M_{pa} = \left(F_y - \frac{\alpha V}{A_g}\right)Z_x = \left(F_y - \frac{\alpha M_A}{e_i A_g}\right)Z_x = \left(1 - \frac{\alpha M_A}{e_i P_Y}\right)M_p \quad (3)$$

Additionally, using the moment diagram of Figure 2, the reduced plastic moment accounting for a reduction due to axial load may be written as
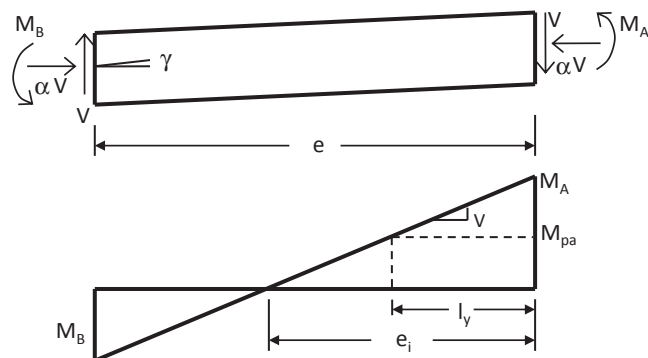
$$M_{pa} = M_A\left(1 - \frac{l_y}{e_i}\right) \quad (4)$$

Setting Equations 3 and 4 equal and solving for the flange yield length gives

$$l_y = e_i\left(1 - \frac{M_p}{M_A}\right) + \frac{\alpha M_p}{P_y} \quad (5)$$

Within the flange yield zone, the average stress is the average of F_{yf} and the flange stress corresponding to moment M_A. To match strain gauge data from tests on links with wide flange sections, Kasai and Popov (1986) modified the average flange stress to be

$$\sigma_{av} = \frac{F_{yf}}{2}\left(1 + \frac{1.1M_A}{M_p}\right) \quad (6)$$

The inelastic plate buckling stress for boundary conditions consistent with that of the flange of a built-up box section—namely, with all edges supported against vertical translation but unrestrained against rotation—was derived by Haaijer (1957) as

$$\sigma_b = \frac{\pi^2}{12}\left(\frac{t_f}{b}\right)^2\left[D_x\left(\frac{b}{l_h}\right)^2 + D_y\left(\frac{l_h}{b}\right)^2 + D_{xy} + D_{yx} + 4G_t\right] \quad (7)$$

where D_x, D_y, D_{xy} and D_{yx} are plastic plate modulii in the longitudinal (x), transverse (y) and shear (xy and yx) directions; G_t is the plastic shear modulus; l_h is the half wavelength of the buckled plate; and b is the free width of the flange. Based on numerous compression tests, Haaijer determined the following values to be appropriate for this modulii: $D_x = 3{,}000$ ksi; $D_y = 32{,}800$ ksi; $D_{xy} = D_{yx} = 8{,}100$ ksi; $G_t = 2{,}400$ ksi. Equation 7 can be used to calculate the plastic flange buckling stress of links with built-up box cross-sections, with the half-wavelength taken as the smaller of the stiffener spacing, or $l_y/2$, where l_y is given by Equation 5. The average flange stress can then be compared with the inelastic plate buckling stress to determine if the flange is likely to buckle.

For shear links, several simplifications and assumptions may be made to reduce the preceding equations to a width-to-thickness limit. First, Haaijer (1957) showed that the minimum plastic buckling stress occurs when

$$\frac{l_h}{b} = 4\sqrt{\frac{D_x}{D_y}} \quad (8)$$

which for the values provided earlier gives $l_h = 0.55b_f$. Using this in Equation 7 gives the minimum plastic buckling stress.

Fig. 2. Link free-body diagram and moment diagram (adapted from Kasai and Popov, 1986).

The maximum average flange stress may be found by estimating the maximum end moment, M_A, for a shear link to be

$$M_A = 1.35 V_p \frac{e}{2} \qquad (9)$$

where e is the total link length and 35% strain hardening is assumed as a reasonable upper bound. The theoretical maximum link length, e^*, for a shear link is

$$e^* = \frac{2M_p}{V_p} \qquad (10)$$

Using Equations 9 and 10 in Equation 6 gives the average flange stress in the flange yield zone to be

$$\sigma_{av} = 1.243 F_{yf} \qquad (11)$$

Limiting the average flange stress in Equation 11 to the plastic buckling stress in Equation 7 and inserting Equation 8 for the half-buckling wavelength, along with the given values for the plastic plate moduli, gives an estimate of the b/t_f for shear links to prevent flange buckling

$$\frac{b}{t_f} \leq \frac{174}{\sqrt{F_{yf}}} = 1.02 \sqrt{\frac{E}{F_{yf}}} \qquad (12)$$

where E is the modulus of elasticity. For flexural links, M_A may be approximated by $1.2M_p$, resulting in an average flange stress of $1.292F_{yf}$ in the flange yield zone and a limiting width-to-thickness ratio of

$$\frac{b}{t_f} \leq \frac{170}{\sqrt{F_{yf}}} = 1.00 \sqrt{\frac{E}{F_{yf}}} \qquad (13)$$

Note that this is different from the b/t_f limit for hollow rectangular sections in the 2010 AISC *Seismic Provisions,* which are

$$\frac{b}{t_f} \leq 0.64 \sqrt{\frac{E}{F_{yf}}} \quad \text{for moderately ductile members} \qquad (14a)$$

$$\frac{b}{t_f} \leq 0.55 \sqrt{\frac{E}{F_{yf}}} \quad \text{for highly ductile members} \qquad (14b)$$

which is the result of work by Lee and Goel (1987) and Hassan and Goel (1991) on fracture and local buckling prevention in concentrically braced frames, based on test results using hollow structural section (HSS) braces. However, the derivation and limits in Equations 12 and 13 do not account for accumulated plastic strain due to cyclic loading. As discussed in the following section, finite element analyses demonstrated that, in many cases, the more restrictive limit of Equation 14a for moderately ductile members was necessary to limit flange local buckling in built-up box links when several cycles of inelastic behavior are considered.

Stiffener Spacing and Web Buckling

Web buckling has also been shown to be an undesirable failure mode for links in EBFs because it causes rapid strength and stiffness degradation. In shear links, the webs are under primarily shear stress, and prevention of web buckling can be achieved through the use of vertical web stiffeners. For shear links of any section, the required stiffener spacing to limit web buckling up to a desired link rotation is a critical design issue. Kasai and Popov (1986) derived the stiffener spacing formula for links with I-shaped sections that appears in the AISC *Seismic Provisions*. The following derivation of a stiffener spacing formula for links with built-up box sections is similar to that for links with I-shaped sections, modified to represent the appropriate web boundary conditions. Note that web width-to-thickness ratio (h/t_w) limits are not directly derived here but are instead based on observations from experiments and finite element analyses as described later.

Kasai and Popov (1986) showed that the required stiffener spacing for shear links could be found by considering the inelastic shear buckling stress, τ_b, given by

$$\tau_b = \eta(\gamma)\tau_E \qquad (15)$$

where $\eta(\gamma)$ is a plastic reduction factor and is a function of the strain history, and τ_E is the elastic shear buckling stress for a plate given by

$$\tau_E = \frac{\pi^2 E}{12(1-\upsilon^2)} K_s(\alpha)\left(\frac{1}{\beta}\right)^2 \qquad (16)$$

where υ is Poisson's ratio; $K_s(\alpha)$ is a buckling coefficient, which is a function of the boundary conditions; and the panel aspect ratio, α, itself is defined as the stiffener spacing, a, over the web depth, $h = d - 2t_f$. Also, β is the web width-to-thickness ratio defined as the web depth over the web thickness, t_w (Basler, 1961).

Kasai and Popov used tests of links with wide flange sections having various yield strengths, aspect ratios, web width-to-thickness ratios and load histories to relate the plastic reduction factor to the secant shear modulus, G_s, and the elastic shear modulus, G, as

$$\eta = 3.7 \frac{G_s}{G} \tag{17}$$

The secant shear modulus is

$$G_s = \frac{\tau_b}{\overline{\gamma}_b} \tag{18}$$

where τ_b is the shear stress at web buckling (the shear force at web buckling divided by the web area), $\overline{\gamma}_b$ is the link rotation from the last point of zero shear force in the load history to the onset of web buckling, and the elastic shear modulus is

$$G = \frac{E}{2(1-\upsilon)} \tag{19}$$

Substituting Equations 16 through 19 into Equation 15, conservatively approximating $\overline{\gamma}_b$ with $2\gamma_u$, where γ_u is the ultimate link rotation, and solving for γ_u gives

$$\gamma_u = 4.35 K_s(\alpha)\left(\frac{1}{\beta}\right)^2 \tag{20}$$

The boundary conditions for the web of a built-up box section may be approximated by assuming the web is hinged along all four sides. This differs from that used for wide flange cross-sections, where it was assumed that the flange provides the web with restraint against rotation. For a shear buckling of a plate with four sides hinged, Galambos (1998) gives $K_s(\alpha)$ as

$$K_s(\alpha) = 5.34 + \frac{4}{\alpha^2} \quad \text{if} \quad \alpha \geq 1 \tag{21a}$$

$$K_s(\alpha) = 4 + \frac{5.34}{\alpha^2} \quad \text{if} \quad \alpha < 1a \tag{21b}$$

Setting the maximum panel aspect ratio α equal to 1, substituting the appropriate expression for $K_s(\alpha)$ into Equation 20 and solving for α gives

$$\alpha = \sqrt{\frac{5.34}{\left(\dfrac{\gamma_u \beta^2}{4.35}\right) - 4}} \tag{22}$$

Note that for panel aspect ratios greater than 1, the constants 5.34 and 4 in Equation 22 switch places. Solving Equation 22 for the stiffener spacing, a, can be conservatively approximated by the following, as discussed in Berman and Bruneau (2005):

$$a = C_B t_w - \frac{h}{8} \tag{23}$$

where C_B is 20 for ultimate link rotations of 0.08 rad and 37 for ultimate link rotations of 0.02 rad. Linear interpolation may be used for other link rotation angles. For I-shaped links, C_B is 30 and 52 for the same ultimate link rotations, respectively. Shear links with built-up box sections having stiffener spacing satisfying Equation 23 should not exhibit web buckling prior to reaching the corresponding ultimate link rotation angle. However, as described later, an upper limit on web-to-thickness ratio is necessary even in the presence of stiffeners. Additionally, for links with large flexural compression stresses in the web, stiffeners alone will likely not prevent web buckling, and a more strict web width-to-thickness ratio limit may be necessary.

EXPERIMENTAL AND ANALYTICAL RESEARCH

This section provides an overview of the research program used to investigate the behavior and ductility of links with built-up box sections and to finalize design recommendations. More detailed discussions of the key components of the research program are available in Berman and Bruneau (2007, 2008a and 2008b). The focus here is to concisely indicate the methods used to finalize the design recommendation for links of this type with an emphasis on the limits for flange width-to-thickness ratio, web width-to-thickness ratio, and stiffener spacing and lateral bracing requirements.

Large-Scale, Single-Story EBF with Built-Up Box Link Test

To investigate the lateral stability and ductility of an EBF with a built-up box link, a large-scale, single-story EBF was tested under quasi-static loading at the University at Buffalo. The test setup and link details are shown in Figure 3. The frame was loaded via a loading beam, and lateral restraint was applied only to the loading beam, thus effectively bracing the columns at the story height against out-of-plane movement. Lateral bracing was not applied to the link, to the beam outside the link, to the braces or along the interstory

column height. The link was designed to be a shear link; using yield strengths obtained from coupon tests for the web and flange steels, the corresponding calculated plastic shear and moment strengths were 111.3 kips and 116.2 kip-ft, respectively, resulting in an $e/(M_p/V_p)$ ratio of 1.43, thus ensuring that the link would behave as a shear link.

Figure 4 shows the experimental results in terms of base shear force versus story drift and link shear force versus link rotation angle. As shown, the link achieved a maximum total link rotation angle of 0.123 rad, which corresponds to an inelastic rotation angle of 0.11 rad for multiple cycles, and achieved a half cycle at a total rotation angle of 0.151 rad. The target plastic rotation angle for the link was the maximum allowed by the AISC *Seismic Provisions* of 0.08 rad, demonstrating that the link had adequate ductility. There was significant link overstrength, as the peak link shear force was 1.5 times the plastic shear force calculated using the material test results. At an inelastic link rotation angle of 0.08 rad, the link shear was 1.39 times the calculated link plastic shear strength. The maximum link moment exceeded the link plastic moment by 8% at the maximum link rotation, further confirming that, in practice, flexure-shear interaction may be neglected due to strain hardening. No evidence of lateral instability was observed, and the maximum out-of-plane moments in the brace members and beam outside the link were, for the most part, less than 2.5% of the link's plastic moment capacity (Berman and Bruneau, 2005). This test demonstrated that EBFs with built-up box sections can develop adequate ductile response without lateral bracing of the link ends.

Note that the 2010 AISC *Seismic Provisions* specify a limit on the ratio of the strong axis to weak axis link moments of inertias, I_x/I_y, to prevent the use of built-up box links with sections that are significantly more susceptible to lateral instability (as well as to ensure sufficient link stiffness out-of-plane of the frame to laterally restrain the braces
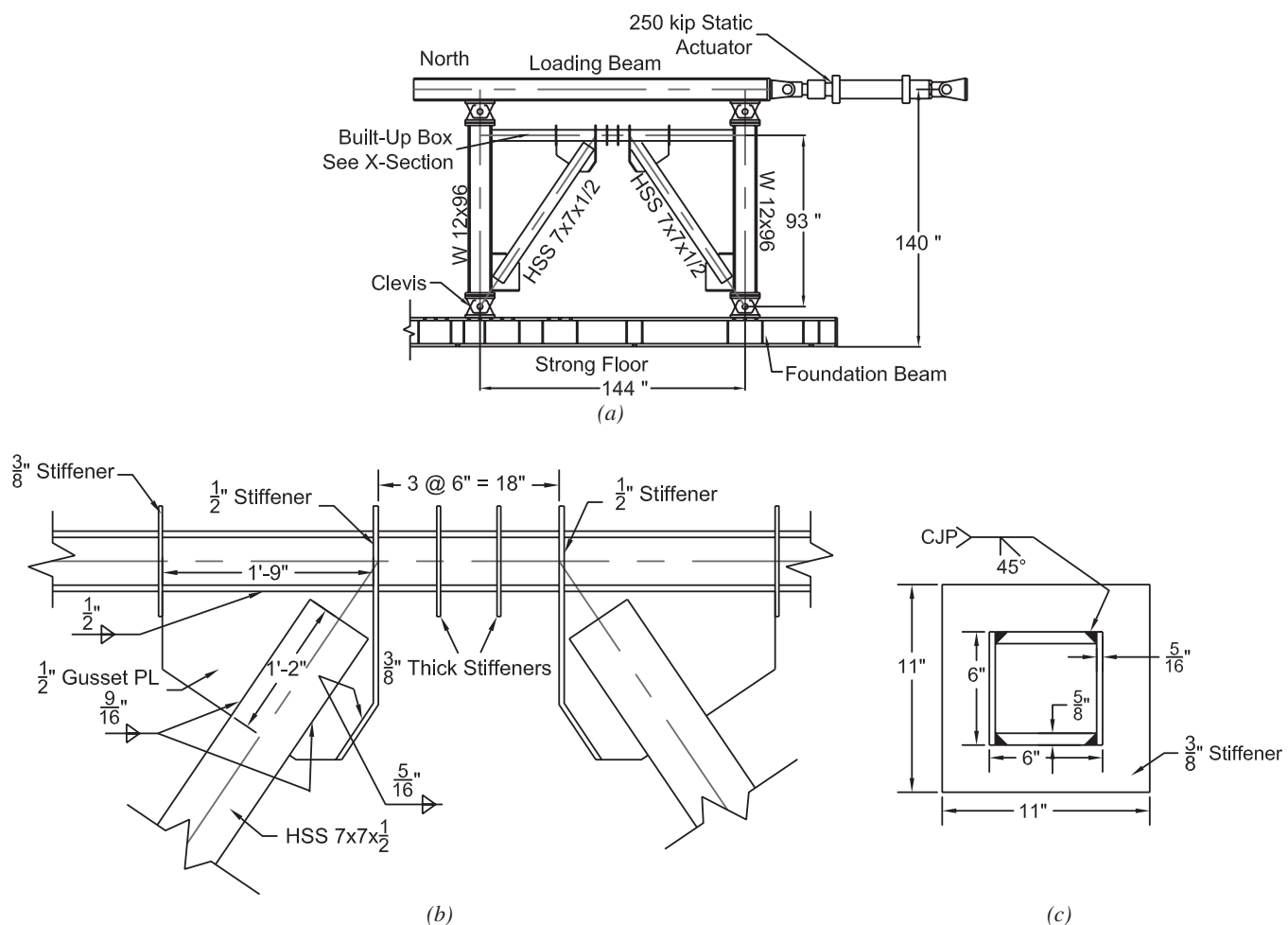

Fig. 3. (a) Large-scale EBF with built-up box link test setup; (b) brace-to-beam connection and link details; (c) link cross-section at stiffeners (adapted from Berman and Bruneau, 2005).

of the eccentrically braced frame). However, it is difficult to achieve links that satisfy the web h/t_w limits discussed later while also having large I_x/I_y. Therefore, in most practical cases, the I_x/I_y, limit is a redundant requirement, and sufficient lateral stability to eliminate the need for lateral bracing of built-up box sections is ensured by simply satisfying the width-to-thickness requirements.

Link Testing and Finite Element Modeling

The b/t_f limits and web stiffener spacing requirements derived earlier do not consider the impact of cyclic inelastic loading. Furthermore, the effect of flexural compression in the webs of intermediate and flexural links necessitates that an upper limit on the web width-to-thickness ratio be used in those cases. To investigate these issues and determine whether the derived requirements are adequate, a series of link finite element analyses and link tests were conducted. A brief overview is provided here, and additional detail can be found in Berman and Bruneau (2008a and 2008b).

The finite element parametric study was conducted in two parts. Part A explored the behavior of links of various cross-sectional dimensions with and without stiffeners and established limits for b/t_f and h/t_w, but used a single material behavior and yield stress. Part B explored the behavior of links with b/t_f and h/t_w at the proposed limits resulting from part A, but with various web and flange yield stresses. All links were modeled using shell elements, and the analyses included material and geometric nonlinearities. The modeling methodology was validated via comparison with the experimental results for the single-story EBF test described briefly earlier and the individual link tests described later.

Each model was subjected to the EBF loading protocol in the 2002 AISC *Seismic Provisions* (AISC, 2002), which specified three cycles at each total link rotation level of 0.0025, 0.005 and 0.01 rad, followed by two cycles at 0.01-rad increments beyond that. That protocol has been demonstrated to be more demanding than the current loading protocol in the 2005 and 2010 AISC *Seismic Provisions* that is based on work by Richards and Uang (2006) and thus should provide conservative results for the plastic rotation capacity of the various links studied. Boundary conditions were applied such that the rotation was restrained at each link end, a vertical displacement was applied at one end of the link corresponding to the target link rotation times the link length, and horizontal translation at the left end was free to prevent the development of link axial force at large rotations. The plastic rotation capacity was taken as the plastic rotation at which the link shear strength had degraded to 80% of the peak strength.

In part A of the finite element parametric study, finite element models were generated for links with lengths of $1.2M_p/V_p$, $1.6M_p/V_p$, $2.1M_p/V_p$ and $3.0M_p/V_p$, having b/t_f values of $0.33\sqrt{E/F_{yf}}$, $0.71\sqrt{E/F_{yf}}$, $1.00\sqrt{E/F_{yf}}$ and $1.66\sqrt{E/F_{yf}}$ (8, 17, 24 and 40, respectively, for $F_{yf} = 50$ ksi) and h/t_w values of $0.50\sqrt{E/F_{yw}}$, $0.66\sqrt{E/F_{yw}}$, $1.00\sqrt{E/F_{yw}}$ and $1.49\sqrt{E/F_{yw}}$ (12, 16, 24 and 36, respectively, for $F_{yw} = 50$ ksi)—all with a flange and web yield stresses of 50 ksi. Both stiffened and unstiffened link models were analyzed for each combination of cross-sectional parameters and lengths, where the stiffeners were external stiffeners (similar to those shown in Figure 1b) that satisfied the spacing requirement of Equation 23.

Results of the part A analyses are summarized in Figure 5. As shown, stiffened and unstiffened links of all lengths with
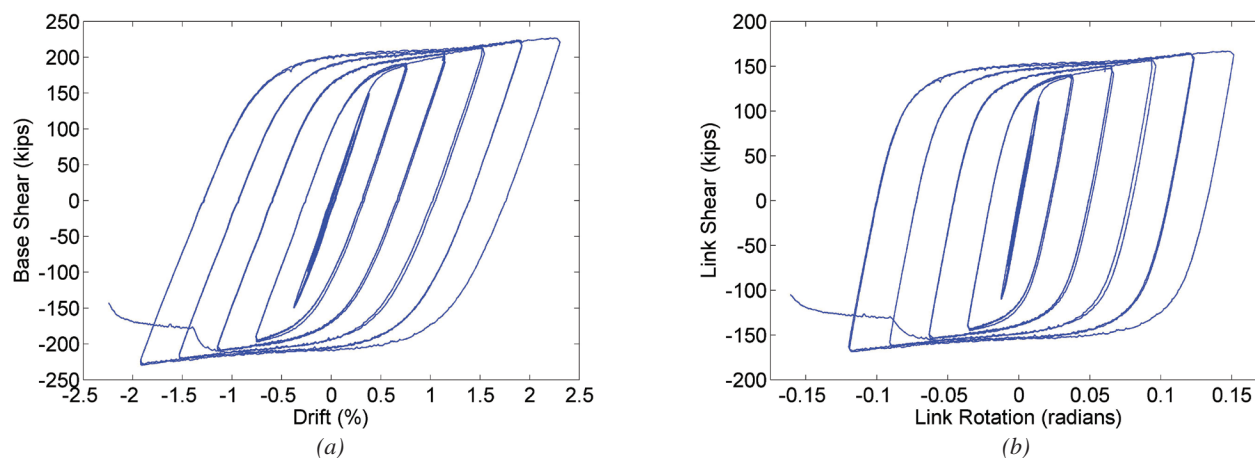

Fig. 4. Large-scale EBF with built-up box link experimental results: (a) base shear versus drift;
(b) link shear force versus link rotation angle (adapted from Berman and Bruneau, 2005).

$b/t_f \leq 0.71\sqrt{E/F_{yf}}$ and $h/t_w \leq 0.66\sqrt{E/F_{yw}}$ had maximum plastic rotations above the limit plastic rotations per the 2002 AISC *Seismic Provisions*, identified as the solid line in the figures. Furthermore, all stiffened links with $e \leq 1.6M_p/V_p$ had maximum plastic rotations above the limit plastic rotations per the 2002 AISC *Seismic Provisions* for all considered h/t_w values when $b/t_f \leq 0.71\sqrt{E/F_{yf}}$. There were three exceptions: two links with lengths of $2.1M_p/V_p$ and one with $1.6M_p/V_p$. The maximum rotations for those links were within 3% of the limit rotations per the 2002 AISC *Seismic Provisions,* and when they were reanalyzed with a slightly larger flange thickness such that $b/t_f = 0.64\sqrt{E/F_{yf}}$, they developed maximum rotations that exceeded the specified limit rotations. Additional analyses described in Berman and Bruneau (2006) were conducted for unstiffened links with $e \leq 1.6M_p/V_p$ and $h/t_w = 1.67\sqrt{E/F_{yw}}$ by increasing the web yield stress. Those links were also found to have adequate plastic rotation capacity. Based on the preceding results, the recommendations for links with built-up box sections in the companion technical note (Bruneau, 2013) were established as follows:

1. All links should have $b/t_f \leq 0.64\sqrt{E/F_{yf}}$.

2. Links with length $e > 1.6M_p/V_p$ do not require stiffeners and should have $h/t_w \leq 0.64\sqrt{E/F_{yw}}$.

3. Links with length $e \leq 1.6M_p/V_p$ should have $h/t_w \leq 1.67\sqrt{E/F_{yw}}$. They may be unstiffened if $h/t_w \leq 0.64\sqrt{E/F_{yw}}$ and should have stiffeners meeting the spacing requirements of Equation 23 if $h/t_w > 0.64\sqrt{E/F_{yw}}$.

Note that flange stiffeners were found to be ineffective in preventing flange buckling. Thus, only web stiffeners are necessary when stiffeners are required, making it possible to place them inside the built-up box section to improve constructability and architectural appeal. Additionally, Figure 5 indicates that for links with lengths greater than $2.1M_p/V_p$, web width-to-thickness ratios greater than $0.66\sqrt{E/F_{yw}}$ are able to achieve their target rotation. An upper bound for web depth-to-thickness for long links was not found as part of this research and could be the subject of future investigation.

Part B of the finite element parametric study consisted of models with webs and flanges proportioned to be just at the upper bounds of the previously recommended plate slenderness limits, with web and flange yield stresses ranging from 36 to 65 ksi. The four link lengths of $1.2M_p/V_p$, $1.6M_p/V_p$, $2.1M_p/V_p$ and $3.0M_p/V_p$ were again considered, and all links were found to have adequate plastic rotation capacity to satisfy the limits in the AISC *Seismic Provisions.*

The preceding recommendations are logical considering the state of stress in the webs and flanges of links with various lengths. For short links, shear yielding of the webs occurs first, and large plastic shear strains in the web require stiffeners to prevent web buckling when h/t_w is large. As strain hardening occurs in the webs, which is more rapid for cyclic shear yielding relative to cyclic yielding under normal stress, the shear force increases, resulting in larger link end moments to maintain equilibrium and correspondingly larger compressive stress in the flanges. Thus, flange buckling is not only a concern for longer links that yield primarily flexure but also for shorter links that yield first in shear. For longer links, the shear stress in the web is lower, and instead, the web may carry considerable flexural compression and tension stresses. Web buckling under this flexural compression is likely for longer links, and vertical web stiffeners are ineffective to prevent such buckling. Therefore, long links require a smaller h/t_w.
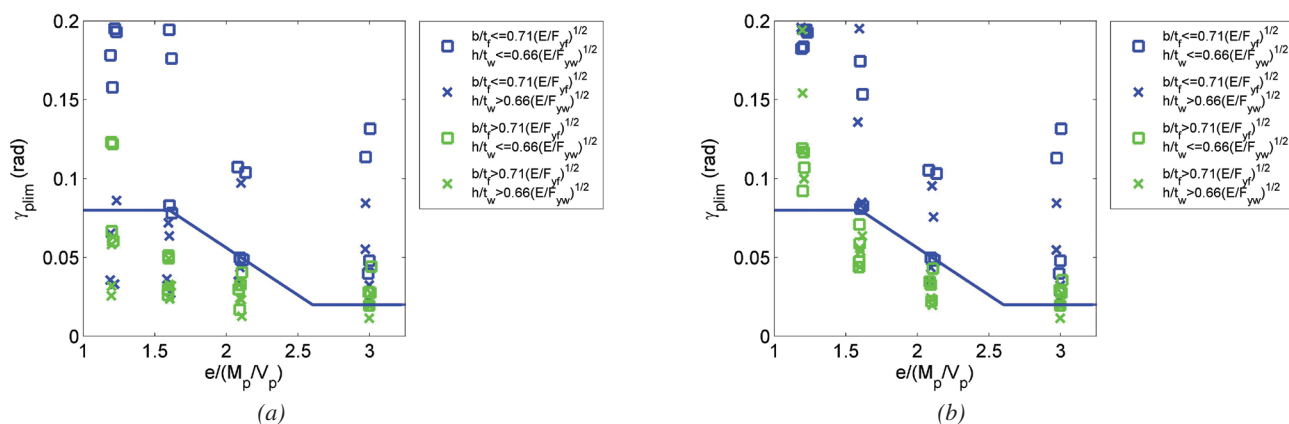

Fig. 5. Finite element modeling results: plastic rotation versus normalized link length for (a) unstiffened links and (b) stiffened links (data from Berman and Bruneau, 2006).

To verify the results of the finite element parametric study, tests on 14 links with built-up box sections were performed and are described in detail in Berman and Bruneau (2008b). The test setup is shown Figure 6 along with the two typical link schematics. Twelve of the links had haunches at their ends to reinforce the connections to the end plates. Two of the links had end details with gusset plates simulating the brace connections used in the full-scale proof-of-concept test, which is a detail more typical of what may be used in an actual EBF implementation. In both cases, the link length is the free length between the end connections as shown in Figure 6.

Flange fracture due to low-cycle fatigue was the governing limit state and the primary cause of strength degradation in all specimens. Although some evidence of moderate web and/or flange buckling was observed in some cases, there was little strength degradation associated with it. This does indicate that flange fracture must be guarded against when detailing the eccentric brace connections to the link, and designers should opt for details that minimize the restraint against flange deformation there. Flange fracture was not simulated in the finite element studies, but a similar failure mode was observed in the full-scale, single-story story test after the link achieved large rotations.

During the testing of the isolated links, the 2005 AISC *Seismic Provisions* were released. They contained a new recommended loading protocol for EBF links based on work by Richards and Uang (2006). The new loading protocol featured more cycles at smaller rotation levels and fewer cycles at larger rotation levels, resulting in less cumulative plastic
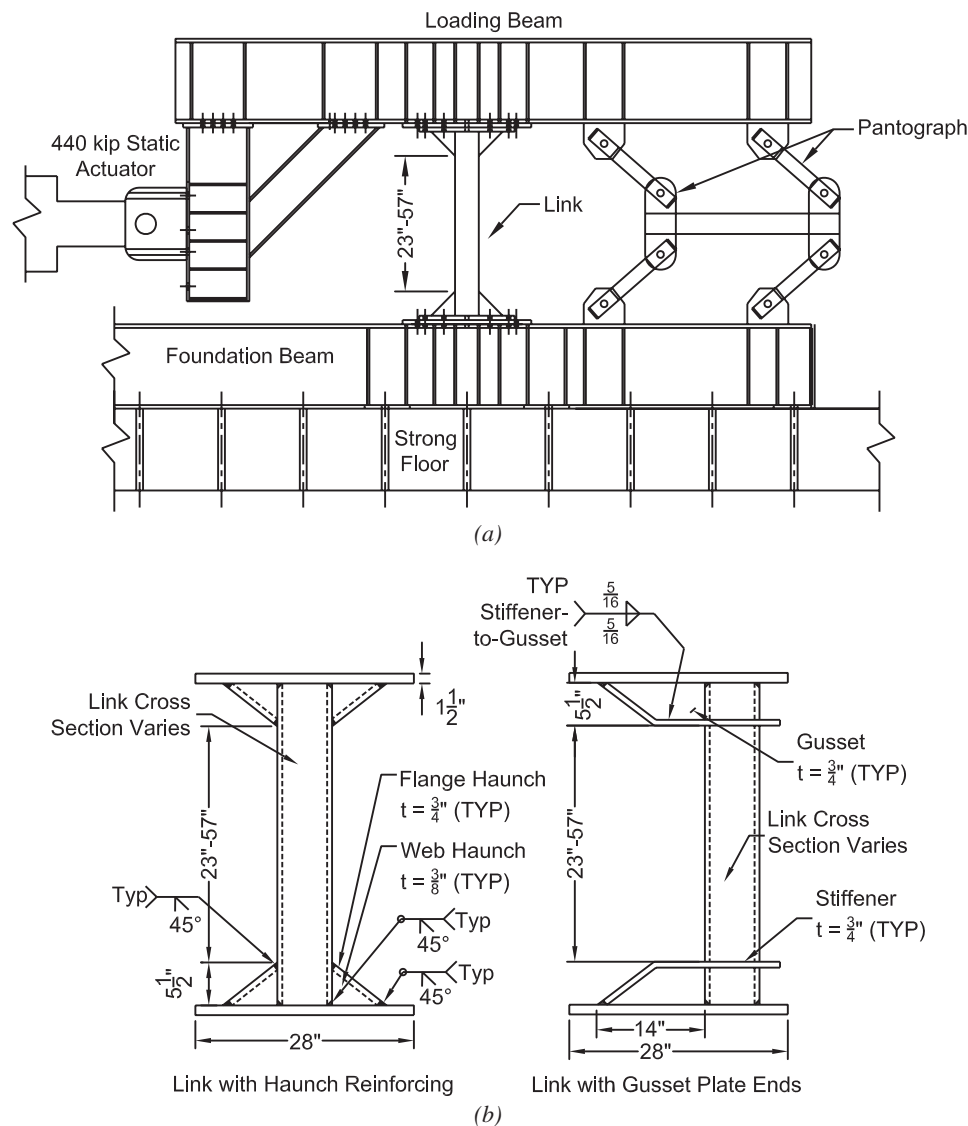

Fig. 6. *Isolated link tests: (a) experimental setup; (b) typical link configurations (adapted from Berman and Bruneau, 2006).*

rotation required to reach the limit plastic rotations. Thirteen of the links were tested under the older, more demanding loading protocol, while one was tested under the newer loading protocol, the latter having identical details as one of the links from the group of 13. The link tested under the new protocol achieved a considerably larger plastic rotation than that achieved with the older loading protocol. The maximum plastic rotations achieved by links tested under the older loading protocol were then projected to maximum plastic rotations that would likely have been achieved under the newer loading protocol using cumulative plastic rotation as the basis for this conversion, as described in Berman and Bruneau (2008b). The resulting projected link plastic rotations are shown in Figure 7 versus the normalized link length, $e/(M_p/V_p)$. The results from the full-scale, single-story EBF test are also included. As shown, all links that meet the proposed design requirements achieved their limit plastic rotations as specified in the 2005 AISC *Seismic Provisions* when the updated loading protocol is considered.

SUMMARY, CONCLUSIONS AND RECOMMENDATIONS

An analytical and experimental study of EBF links built-up box sections was performed to develop design recommendations, including lateral bracing conditions, flange width-to-thickness and web width-to-thickness limits, and stiffener spacing requirements. The study consisted of a derivation of some design requirements, large-scale testing of a single-story EBF with a built-up box link, a parametric study using finite element analyses of built-up box links with various section dimensions, and an experimental study on isolated links having various sections properties and plate slenderness ratios. In general, links with built-up box sections performed adequately and were able to meet the ductility requirements for use in EBFs, as long as the proposed width and width-to-thickness ratio limits were satisfied.

A flange width-to-thickness ratio limit was derived considering plate buckling equations, but it was shown to be unconservative by finite element analysis results that considered cyclic plastic deformation of the flanges. Web stiffener spacing requirements were derived using methods similar to those used for stiffener requirements for links with I-shaped sections and were found to be adequate by the results from the finite element analyses and experiments. An upper limit on web width-to-thickness ratio was established via the finite element parametric study. Lateral bracing was not used for the link or beam in the full-scale, single-story EBF test, and no evidence of lateral instability was observed. Based on the cumulative results of the study, the design requirements for EBF links with built-up sections are:

1. All links should have $b/t_f \leq 0.64\sqrt{E/F_{yf}}$.

2. Links with length $e > 1.6M_p/V_p$ do not require stiffeners and should have $h/t_w \leq 0.64\sqrt{E/F_{yw}}$.

3. Links with length $e \leq 1.6M_p/V_p$ should have $h/t_w \leq 1.67\sqrt{E/F_{yw}}$. They may be unstiffened if $h/t_w \leq 0.64\sqrt{E/F_{yw}}$ and should have web stiffeners if $h/t_w > 0.64\sqrt{E/F_{yw}}$.
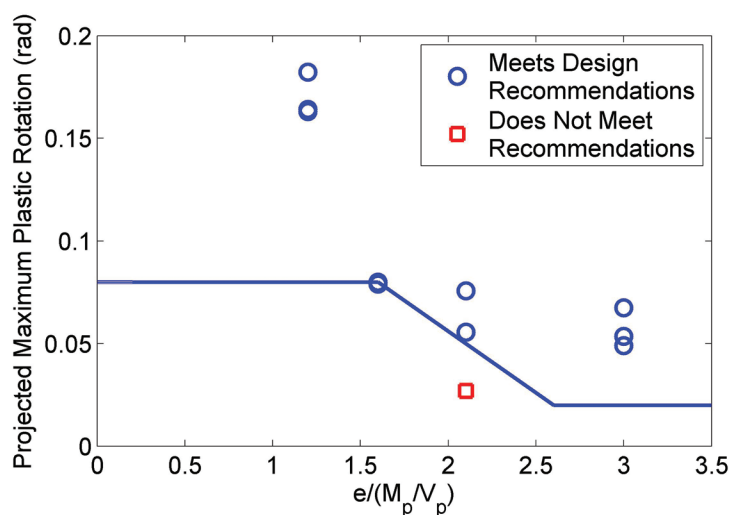

Fig. 7. Isolated link test results, projected maximum plastic rotation versus normalized link length (data from Berman and Bruneau, 2006).

4. Where web stiffeners are required they should be spaced at a spacing, a, no larger than:

$$a = C_B t_w - \frac{h}{8} \qquad (23)$$

where C_B is 20 and 37 for maximum link rotations of 0.08 and 0.02 rad, respectively. Linear interpolation may be used for other link rotation angles.

5. Lateral bracing of links with built-up box sections is unlikely to be necessary.

ACKNOWLEDGMENTS

REFERENCES

AISC (2002), *Seismic Provisions for Structural Steel Buildings,* AISC 341-02, American Institute of Steel Construction, Chicago, IL.

AISC (2005), *Seismic Provisions for Structural Steel Buildings,* AISC 341-05, American Institute of Steel Construction, Chicago, IL.

AISC (2010), *Seismic Provisions for Structural Steel Buildings,* AISC 341-10, American Institute of Steel Construction, Chicago, IL.

Basler, K., (1961), "Strength of Plate Girders in Shear," *Journal of the Structural Division*, ASCE, Vol. 87, No. 7, pp. 150–180.

Berman, J.W. and Bruneau, M. (2005), "Approaches for the Seismic Retrofit of Braced Steel Bridge Piers and Proof-of-Concept Testing of a Laterally Stable Eccentrically Braced Frame," Technical Report No. MCEER-05-0004, Multidisciplinary Center for Earthquake Engineering Research, Buffalo, NY.

Berman, J.W. and Bruneau, M. (2006), "Further Development of Tubular Eccentrically Braced Frame Links for the Seismic Retrofit of Braced Steel Truss Bridge Piers," Technical Report No. MCEER-06-0006, Multidisciplinary Center for Earthquake Engineering Research, Buffalo, NY.

Berman, J.W. and Bruneau, M. (2007), "Experimental and Analytical Investigation of Tubular Links for Eccentrically Braced Frames," *Engineering Structures*, Vol. 29, No. 8, pp. 1929–1938.

Berman, J.W. and Bruneau, M. (2008a), "Tubular Links for Eccentrically Braced Frames I: Finite Element Parametric Study," *Journal of Structural Engineering*, ASCE, Vol. 134, No. 5, pp. 692–701.

Berman, J.W. and Bruneau, M. (2008b), "Tubular Links for Eccentrically Braced Frames II: Experimental Verification," *Journal of Structural Engineering*, ASCE, Vol. 134, No. 5, pp. 702–712.

Bruneau, M. (2013), "Setting Limits," *Modern Steel Construction,* February.

Galambos, T.V. (1998), *Guide to Stability Design Criteria for Metal Structures*, John Wiley and Sons, New York, NY.

Haaijer, G. (1957), "Plate Buckling in the Strain-Hardening Range," *Journal of the Engineering Mechanics Division*, Vol. 83, No. 2, pp. 1212-1 – 1212-47.

Hassan, O.F. and Goel, S.C. (1991), "Modeling of Bracing Members and Seismic Behavior of Concentrically Braced Steel Structures," Technical Report UMCE 91-1, University of Michigan Department of Civil Engineering, Ann Arbor, MI.

Kasai, K. and Popov, E.P. (1986), "Study of Seismically Resistant Eccentrically Braced Steel Frame Systems," Report No. UCB/EERC-86/01, Earthquake Engineering Research Center, College of Engineering, University of California, Berkeley, CA.

Lee, S. and Goel, S.C. (1987), "Seismic Behavior of Hollow and Concrete-Filled Square Tubular Members," Technical Report UMCE 87-11, University of Michigan Department of Civil Engineering, Ann Arbor, MI.

Richards, P. and Uang, C. M. (2006). "Testing Protocol for Short Links in Eccentrically Braced Frames," *Journal of Structural Engineering*, ASCE, Vol. 132, No. 8, pp. 1183–1191.

Roeder, C.W. and Popov, E.P. (1977), "Inelastic Behavior of Eccentrically Braced Steel Frames Under Cyclic Loadings," Report No. UCB/EERC-77/18, Earthquake Engineering Research Center, College of Engineering, University of California, Berkeley, CA.